

# EVALUATION OF RADOME PERFORMANCE FROM CYLINDRICAL NEAR-FIELD MEASUREMENTS

W.C. Dixon & Daniël Janse Van Rensburg\*  
Chelton Radomes Ltd.,  
Six Hills Way, Stevenage, SG1 2DH, United Kingdom  
Tel: +44 1438 768859  
Fax: +44 1438 76 8844  
e-mail: [bill.dixon@radomes.co.uk](mailto:bill.dixon@radomes.co.uk)

\*Nearfield Systems Inc, 19730 Magellan Drive, Torrance, CA 90502-1104, USA  
Tel: (613) 270 9259  
Fax: (613) 2709260  
e-mail: [drensburg@nearfield.com](mailto:drensburg@nearfield.com)

## Abstract

This paper describes the installation and implementation of a Cylindrical Near-field Test Facility at Chelton Radomes Ltd, Stevenage, (formerly British Aerospace Systems and Equipment Ltd.), in the UK for the testing of large radome/antenna combinations. Test site commissioning and validation activities to determine measurement accuracy & repeatability for the radome performance parameters of transmission loss and boresight error, are discussed. Test data from actual measurements are presented.

**Keywords:** Cylindrical Near-field testing, Radomes.

## 1. INTRODUCTION

Traditionally, measurement of the radiation characteristics of antennas has used far-field and compact antenna ranges. This is particularly true when measuring antenna performance when enclosed by a radome. If the antennas/radomes being tested are physically (and electrically) large (many tens or even hundreds of wavelengths), then there are certain constraints:

- a) A traditional far-field range would require a significant amount of real estate, due to the separation distance between transmit and receive antennas.
- b) A compact antenna range would require a large reflector, producing a test zone large enough to accommodate the antenna/radome.

There has been significant growth in the use of near-field measurement systems in recent years and there are now numerous test facilities around the world measuring a variety of antennas for different applications using planar, cylindrical and spherical near-field measurement techniques. This is due, in part, to the data storage capacity and speed of modern personal computers, which can acquire and process the large volume of data, associated with near-field antenna measurements, in acceptable time scales.

The evaluation of antenna performance, when enclosed by a radome presents no significant variations from the bare antenna case. The main difference being the additional hardware required to accommodate the radome.

Near-field techniques can therefore be utilized to examine the perturbation of the antenna radiation characteristics due to the presence of the radome [1].

A comparison of the available near-field techniques was made in order to select the most suitable for measuring a large airborne antenna system and associated radome. From this comparison the cylindrical measurement technique was the preferred option for the following reasons:

- i) Reduced measurement time compared to the planar technique in order to obtain the same far-field coverage in the reconstructed patterns.
- ii) Reduced costs and complexity for the antenna/radome mounting and interface hardware when compared to the needs for a spherical system.

Both i) and ii) above apply to the specific antenna/radome system considered here and should not be regarded as general statements. A more detailed discussion on the relative merits of the various near-field measurement techniques can be found in [2].

When a radome is installed over a particular antenna system, the radiation characteristics of that antenna are modified. These changes affect the beam-pointing angle, reduce the gain of the antenna and modify the side lobe structure of the far-field radiation pattern. The degree by which these parameters are affected is a function of the relative orientation of the antenna within the radome and the operating frequency of the radar.

The design of the radome can be optimized to reduce the effects of a particular parameter, e.g. beam pointing (boresight) error, but in general, the effects cannot be eliminated.

This paper describes the implementation of the cylindrical near-field measurement facility at Chelton Radomes Ltd (CRL), to determine the boresight error and transmission loss performance of a large airborne radome.

## 2 DESCRIPTION OF TEST FACILITY

### 2.1 Hardware

#### 2.1.1 Near-Field Scanner System

A photograph of the measurement facility is shown in Figure 1. (Unfortunately for commercial reasons the antenna itself cannot be shown.)



**Figure 1:** Combined Planar/Cylindrical Scanner.

The measurement system is a combined planar/cylindrical system, however, only the cylindrical option is used in this instance. This is an off the shelf system supplied by Nearfield Systems Incorporated (NSI). The planar scanner has a scan area of 2.4m x 2.4m. The 2.4m vertical height provides sufficient coverage to determine the antenna elevation plane radiation pattern even when at the extreme scan angles, without the need to re-position the main beam parallel to the site axis. The measurement parameters being evaluated are functions of the main beam characteristics and hence only a limited portion of the radiation pattern is required.

The azimuth rotary stage (required for the cylindrical option) is a custom made device, also manufactured by NSI. Figure 2 shows the probe antenna used to sample the electromagnetic field radiated by the antenna under test (AUT). This is a corrugated horn antenna with a very large flare angle. The probe incorporates an Orthomode Transducer (OMT) and with the addition of an independent PIN diode switch, vertical and horizontal polarization components to be measured almost simultaneously.



**Figure 2:** Probe antenna aperture.

The probe mounts on to the carriage on the vertical tower of the planar scanner, which can travel at speeds up to 0.25m/s.

### 2.1.2 Antenna Under Test and Interfacing Hardware

The AUT comprises a shaped reflector antenna, designed to produce a fan beam in the elevation plane and a  $\sin(x)/x$  characteristic in the azimuth plane. The reflector moves independently of the feed assembly to allow beam scanning to be performed. The beam-pointing angle is therefore approximately twice the introduced mechanical angle. The complete antenna system (i.e. reflector, mounting yoke and servo housing) is mounted on to the azimuth rotary stage using a custom designed interface structure. This structure allows the antenna system to be rotated  $360^\circ$  independently of the rotary stage. The antenna is positioned at a particular azimuth angle and located using a spring-loaded pin, which locks in one of the precision-drilled holes in the mounting structure. The antenna attachment/ positioning hardware is installed on a sub-structure that also accommodates the radome. The relative geometry of these two structures is such that the position of the antenna swept volume, within the radome, is representative of the actual aircraft installation.

Movement of the reflector in the elevation plane is achieved using a linear actuator, which is driven by a stepper motor. This device is mounted behind the antenna and is attached to the rear of the reflector via a solid metal link. The movement of the reflector is fully automated, via software run on the system workstation.

The azimuth rotary stage, radome interface structure and antenna mounting hardware are mounted on a platform in order to raise the equipment and locate the elevation gimbal axis close to the mid point of the probe vertical travel range.

### 2.1.3 Measurement System Receiver

An Agilent 8530A is used as the system receiver. An averaging factor of 32 is used in order to improve measurement stability. A schematic diagram of the measurement system equipment is shown in Figure 3.

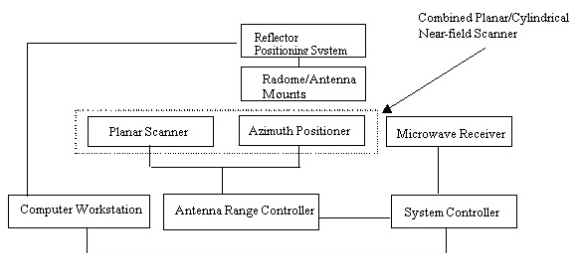


**Figure 3:** Simplified System Block Diagram

### 2.1.4 Measurement Geometry

The relative geometry of the radome, AUT and probe antenna is shown in Figure 4.

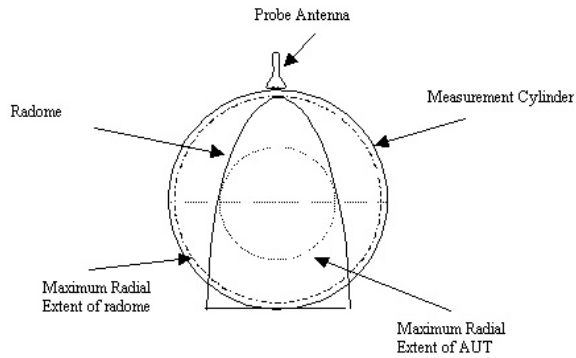


**Figure 4: Radome/Measurement Cylinder Geometry**

The separation distance between the probe and the nose of the radome is governed by the clearance required to avoid a collision between the probe and the rear of the test component when acquiring data with the antenna at the maximum azimuth angle.

The main point to note from this figure is that the maximum radial extent of the radome replaced the maximum radial extent of the AUT as the input to the software.

## 2.2 Software

Positioning of the probe, azimuth rotary stage and antenna reflector is controlled via the measurement system computer workstation. Proprietary software [3] purchased with the scanner system, coordinates probe antenna and rotary stage movement together with the acquisition of electromagnetic field data via the system receiver.

Details such as the antenna shape and size, far field angular coverage and measurement radius are entered into the software by the user, which is used by the software to calculate the sampling interval etc.

It has a powerful in-built scripting language, which can be used to customize the measurement system by allowing communication /control of external devices associated with the measurement system (e.g. for this measurement system the reflector of the AUT).

## 3. SITE VALIDATION

An exercise was undertaken to evaluate the accuracy of the measurement system. This examined mechanical (azimuth rotary stage and AUT reflector positioning system) and electrical (radome performance) aspects of the facility. This exercise was conducted at a single frequency, for vertical polarization only. In both instances repeatability is very important as radome performance is derived from two antenna measurements i.e. with and without the presence of the radome.

From this work the positional repeatability of the azimuth rotary stage was found to be  $\pm 0.006^\circ$ , and  $\pm 0.002^\circ$  for the reflector positioning system.

Absolute accuracy for the described radome performance parameters was determined, again at a single frequency and for vertical polarization. Transmission loss was evaluated over the range 0 to  $-5\text{dB}$  whilst boresight error was evaluated over  $\pm 10\text{mrad}$ . The resulting measurement accuracy for transmission loss is  $\pm 0.075\text{dB}$ , whilst for boresight error it is  $\pm 0.1\text{mrad}$ .

A further series of tests was carried out, with the antenna located at the same look angle, (with the radome present) in order to evaluate measurement repeatability. The measurement system has been designed to perform measurements at seven antenna elevation angles, for a given azimuth angle. For the repeatability measurements the seven elevation look angles were selected to be the same i.e.  $0^\circ$ . The azimuth angle was also selected to be  $0^\circ$ .

The series of tests was conducted twice, giving a total of 14 measurements in order to evaluate measurement repeatability.

In addition, a further three measurements were carried out, where the radome was installed and removed for each measurement to examine the effects (if any), due to the loading/ removal of the radome. The resulting performance data is shown in Table 1. The total spread of azimuth boresight error, for all the above measurements ranged from  $0.052\text{mrad}$  to

0.122mrad i.e. a maximum variation of 0.07mrad. For the elevation boresight error case, the total spread was approximately 0.1mrad. The corresponding variation of transmission loss performance ranged from 0.46 dB to 0.51 dB.

| Cycle | Azimuth<br>BSE<br>(mrad) | Elevation<br>BSE<br>(mrad) | Tx.<br>Loss<br>(dB) |
|-------|--------------------------|----------------------------|---------------------|
| 1     | 0.070                    | 0.000                      | 0.472               |
| 2     | 0.122                    | 0.000                      | 0.493               |
| 3     | 0.122                    | 0.105                      | 0.472               |
| 4     | 0.070                    | 0.000                      | 0.447               |
| 5     | 0.122                    | 0.000                      | 0.460               |
| 6     | 0.122                    | 0.000                      | 0.467               |
| 7     | 0.070                    | 0.000                      | 0.462               |
| 8     | 0.070                    | 0.000                      | 0.462               |
| 9     | 0.070                    | 0.000                      | 0.473               |
| 10    | 0.070                    | 0.000                      | 0.464               |
| 11    | 0.087                    | 0.000                      | 0.523               |
| 12    | 0.052                    | 0.000                      | 0.505               |
| 13    | 0.105                    | 0.000                      | 0.499               |
| 14    | 0.052                    | 0.105                      | 0.487               |
| 15    | 0.052                    | 0.105                      | 0.491               |
| 16    | 0.052                    | 0.000                      | 0.481               |
| 17    | 0.052                    | 0.105                      | 0.498               |

**Table 1:** Radome Performance Repeatability

This level of repeatability is excellent, given the number of measurement sequences, the fact that the reflector position changes between measurements and the 15-hour duration between the start of the first and final measurement sequence.

#### 4. FURTHER RADOME MEASUREMENTS

Having completed the exercises described above, a more structured set of tests was carried out. This testing comprised the Product Acceptance Test (PAT) regime for this particular component. From these tests, it would be possible to examine the performance characteristics as a function of antenna look angle and frequency. For the purpose of these tests a second radome was used (production standard unit).

Figures 5 and 6 show transmission loss vs. antenna azimuth look angle performance for horizontal and vertical polarization respectively. These figures show three curves, identified as Fl, Fm and Fh which correspond to the lower, center and upper operating frequencies of the radar system.

An examination of these figures shows peak loss occurring when the antenna is at 0° azimuth i.e. when the antenna is looking through the nose of the radome. This is typical for an aerodynamic shape. The radome is symmetrical in the azimuth plane and therefore one would expect this to be reflected in the shape of the curves in Figures 5 and 6. This is true to a large extent, however, the curves do exhibit some asymmetric features for negative antenna scan angles, which occur for both polarizations. Peak loss is around 0.9dB (at 0° azimuth). For both polarizations, the maximum loss reduces as the frequency is increased suggesting that, at this particular antenna angle, the radome is tuned for the higher frequency.

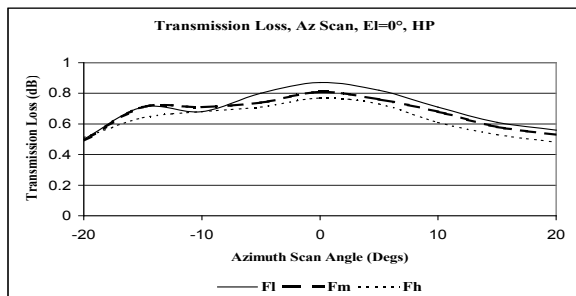


**Figure 5:** Transmission Loss vs. Azimuth Look Angle- Horizontal Polarization.

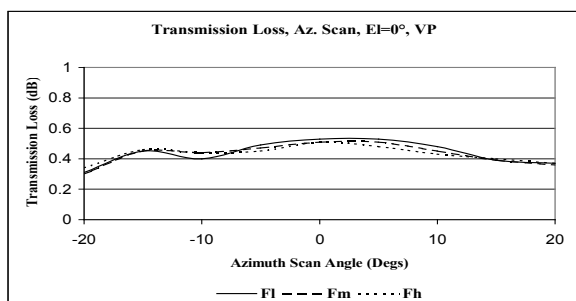


**Figure 6:** Transmission Loss vs. Azimuth Look Angle- Vertical Polarization.

Figures 7 and 8 show the azimuth boresight error characteristic for horizontal and vertical polarization, respectively. These plots have been included to show the peak values for this parameter.

Figure 7 shows a classic boresight characteristic. There is no (or very little) boresight error when the antenna is looking dead ahead i.e.  $0^\circ$  and the curves show the degree of symmetry one would expect due to the symmetrical shape of the radome in this plane. The features observed at the negative antenna angles in the transmission loss plots are clearly not evident here, suggesting that they are real and not due to measurement or systematic error.

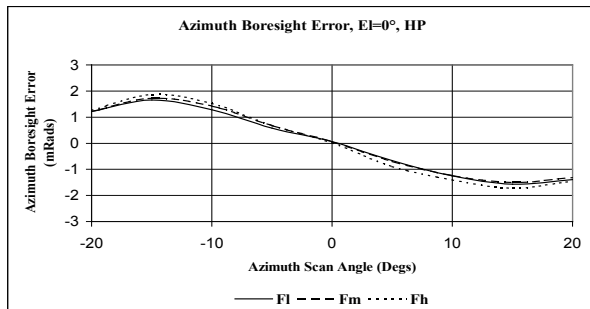


**Figure 7:** Azimuth Boresight Error vs. Azimuth Scan Angle- Horizontal Polarization.

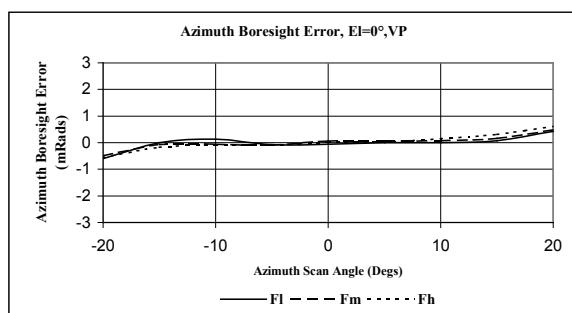


**Figure 8:** Azimuth Boresight Error vs. Azimuth Scan Angle- Vertical Polarization.

Peak values occur when the antenna is scanned a little way off the radome axis of symmetry, in this case when the antenna is located at approx.  $\pm 15^\circ$ , resulting in a peak value of around 2mrad. This, value increases with frequency, over the band of interest i.e. from F1 to Fh.

The response for vertical polarization in Figure 8 also shows the expected symmetrical characteristic, but is generally 'flatter', with a lower peak value of around 0.5mrad. Again there is no evidence of the ripple found in the transmission loss plots for negative antenna look angles.

Figures 9 and 10 show the elevation plane boresight error for horizontal and vertical polarization respectively. Due to the operation of the reflector in this plane the measured boresight error has been plotted as a function of the introduced mechanical angle. The asymmetric characteristic, evident in both figures, is attributable to the asymmetric shape of the radome in the elevation plane. For the case of horizontal polarization the peak value is approximately 7.5mrad and occurs at an elevation angle of  $3^\circ$ . The peak value for vertical polarization is a little over -2mrad.

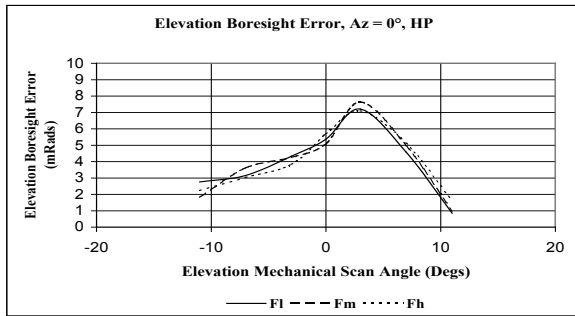


**Figure 9:** Elevation Boresight Error vs. Mechanical Reflector Angle, Horizontal Polarization.

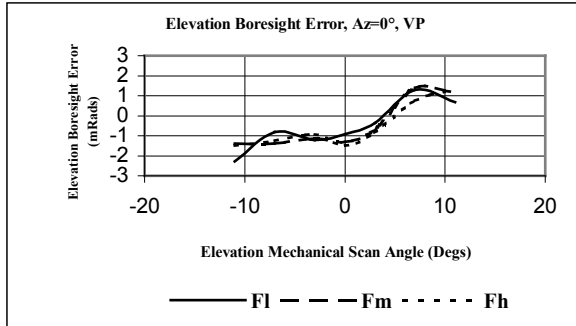


**Figure 10:** Elevation Boresight Error vs. Mechanical Reflector Angle, Vertical Polarization.

## 5. CONCLUSIONS

A cylindrical near-field measurement system is now in use at Chelton Radomes Ltd., Stevenage for the purpose of measuring the electrical performance of a large airborne radome. Formal qualification testing has been completed and the facility is in use for radome production qualification.

The near-field measurement technique has proved to be extremely useful for measuring large antenna/radome combinations, The main advantages are reduced real estate requirements, environmentally controlled test chambers and automated data acquisition/processing, thus allowing 24 hour measurement capability.

The results reported here have been very encouraging and have prompted further and significant investment into the near-field test facilities at Chelton Radomes Ltd. A second cylindrical system, with a 6.7m vertical scan height has been procured and installed. This facility is currently utilized for measuring the electrical performance of two large airborne radomes, for helicopter and satellite communication applications.

## 6 REFERENCES

- [1] E.B. Joy, "Microwave holography for antenna and radome diagnostics", Antennas and Propagation Society, 2001 IEEE International Sym , Volume: 4 , 2001, pp. 440 –443.
- [2] Paul F. Wacker and Allen C. Newell, "Advantages and disadvantages of Planar, Circular Cylindrical and Spherical Scanning and Description of the NBS Antenna Scanning Facilities"- ESA SP127- "Antenna Testing Techniques", May 1977.
- [3] *NSI2000 Software Users Manual*, Nearfield Systems Inc, Torrance, CA, USA, 2002